Integrated Motor Drive Design for an All-Electric Boat

Conference Paper · October 2014

DOI: 10.13140/2.1.4589.0245

5 authors, including:

Thiago B. Soeiro
Delft University of Technology

Marcos J. Jacoboski
Federal University of Santa Catarina

M.L. Heldwein
Federal University of Santa Catarina

Arnaldo José Perin
Federal University of Santa Catarina

Integrated Motor Drive Design for an All-Electric Boat

Fuerback, André L., INEP – UFSC, Brazil, andre.fuerback@gmail.com
Soeiro, Thiago B., ABB – PEG, Switzerland, thiago-batista.soeiro@ch.abb.com
Jacoboski, Marcos J., INEP – UFSC, Brazil, marcosjose@inep.ufsc.br
Heldwein, Marcelo L., INEP – UFSC, Brazil, marcelo.heldwein@gmail.com
Perin, Arnaldo J., INEP – UFSC, Brazil, arnaldo.perin@gmail.com

Abstract

This work describes a packaging solution to the electric propulsion motor drive of an all-electric boat. In order to derive a compact drive system the power inverter and cooling apparatus are integrated with the electric propulsion motor. Therefore, the full system fits directly into the power head of an outboard motor boat. The system main parts are a permanent magnet synchronous machine (PMSM), a MOSFET-based inverter, a water cooling heat sink and an onboard control system based on a digital signal controller.

1 Introduction

Among the various environmental problems faced today, water pollution caused by navigation is a concern, mainly in tourist areas where the traffic is increasing every year, but also in environmentally protected areas. Initiatives to use electrical propulsion systems in transportation represent alternatives to reduce the environment pollution and improve overall life quality standards, among other benefits [1-3].

Fig. 1 presents the electric diagram of the all-electric boat referred in this work, which has a capacity for carrying 2 people plus load on board. The boat is driven by two 10 kW permanent magnet synchronous motors (PMSM) powered by a lithium-ion battery bank. The battery bank is composed of 30 cells of Lithium Iron Phosphate (LiFePO 4) providing enough energy for approximately one hour and twenty-five minutes at the maximum power of 20 kW or five hours when cruising at lower speeds, i.e. at 5 kW. In order to increase the system cruise range 1.4 m^2 of photovoltaic (PV) panels providing up to 9.6% of the rated power is installed on the roof of the boat. The batteries are also recharged through a dedicated charging station located on the harbor or docks while the boat is moored. This is grid-connected, and can also be connected to a local PV array.

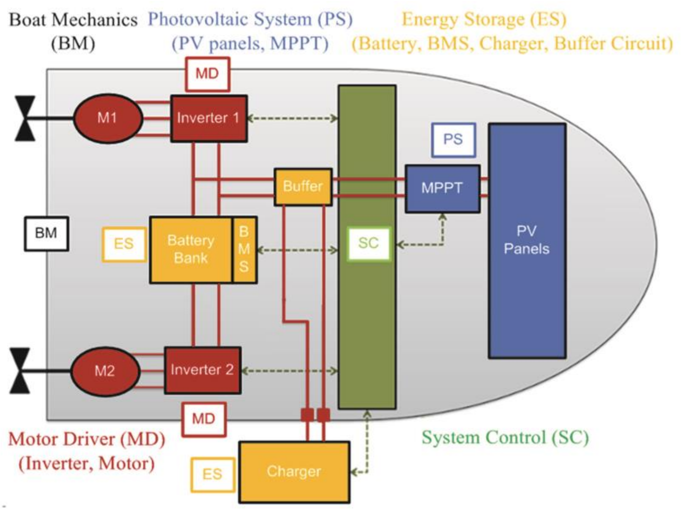

Fig. 1: Electric diagram of the all-electric boat.

This work describes the main components of an integrated motor drive system (IMDS) to propel an all-electric boat. The developed highly compact IMDS fits directly into the power head of an outboard motor boat. The main parts of the system are presented in the followings.

2 Propulsion Integrated Motor Drive System

Each electric motor as well as the power converter of the drive system is to be installed in the power head of a commercial outboard motor (Fig. 2). This brings simplicity and versatility to the solution, allowing it to be installed on virtually any boat driven by an outboard motor. This section describes the proposed IMDS [4-6].

(a) commercial 15HP outboard; (b) mechanical – power train; (c) electrical – power train.

Fig. 2: Electric propulsion system.

The electric propulsion motor consists of a permanent magnet synchronous machine designed within the project framework. The main characteristics of the designed PMSM are listed in Tab. I.

Tab. I: Main specifications of the developed permanent magnet synchronous motor.

Mechanical torque on shaft	20 N.m
Rated current per phase	85 Arms
Mechanical power on shaft	10.5 kW
Speed	5,000 rpm
Copper losses at room temperature	119 W
No-load losses (at 5.000 rpm and room temp.)	228 W
Total losses (estimated at room temp.)	347 W
Efficiency	96.7 %

The machine and subparts, such as the rotor and stator, are highlighted in Fig. 3.

(a) PMSM assembled; (b) stator; (c) rotor;

Fig. 3: Permanent magnet synchronous motor.

2.1 Integrated Drive Power Inverter

The voltage source inverter (VSI) selected to drive each 10 kW PMSM is shown in Fig. 4. The main converter specifications are given in Tab. II. The power converter comprises a two-level VSI constructed with MOSFET power modules from Microsemi (APTM20AM04FG). Due to the low dc-link voltage silicon MOSFETs are well suited for this application.

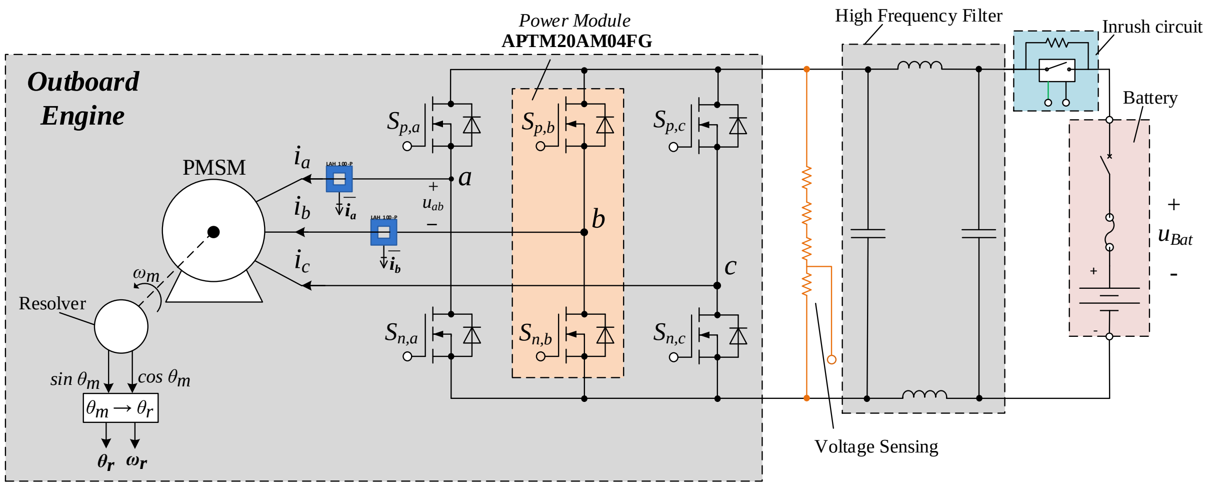

Fig. 4: Propulsion system power structure.

For driving the PMSMs, field-oriented control (FOC) is applied in order to achieve zero *d*-axis current control (ZDAC) and consequently minimize overall conduction losses (cf. Fig. 5). An on-board Texas Instruments floating point TMS320F28069 digital signal controller is used to implement the FOC and the sinusoidal PWM (SPWM) modulation used to drive the MOSFETs.

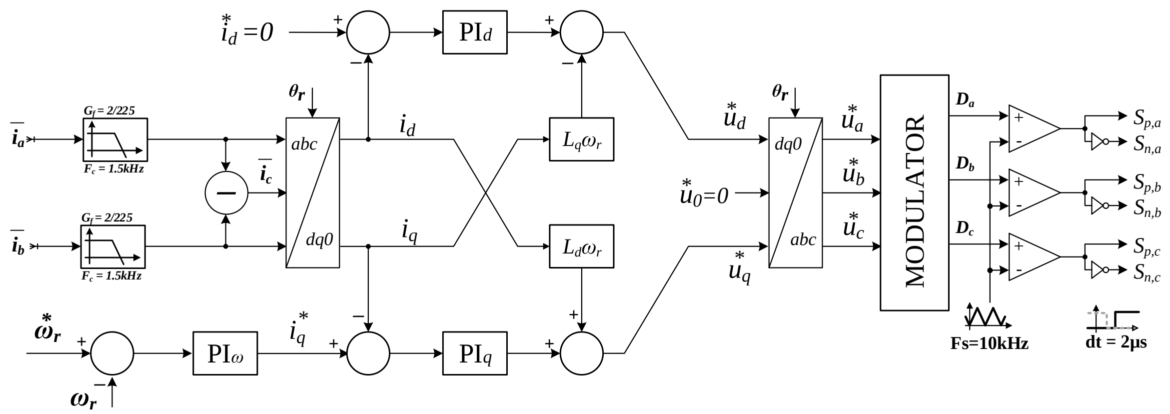

Fig. 5: Control strategy.

The switch gate driver, providing insulation between the power stage and control circuits, is shown in Fig. 6. There, an isolated circuit operating at high frequency (nearly 500 kHz) is used to produce the isolated auxiliary dc 15 V and 5 V required in the main gate driver circuit. In order to complete the propulsion system, protection circuits and a high frequency filter are added to the system. The latter is used to limit the current ripple injection into the battery bank. The constructed prototype is shown in Fig. 7.

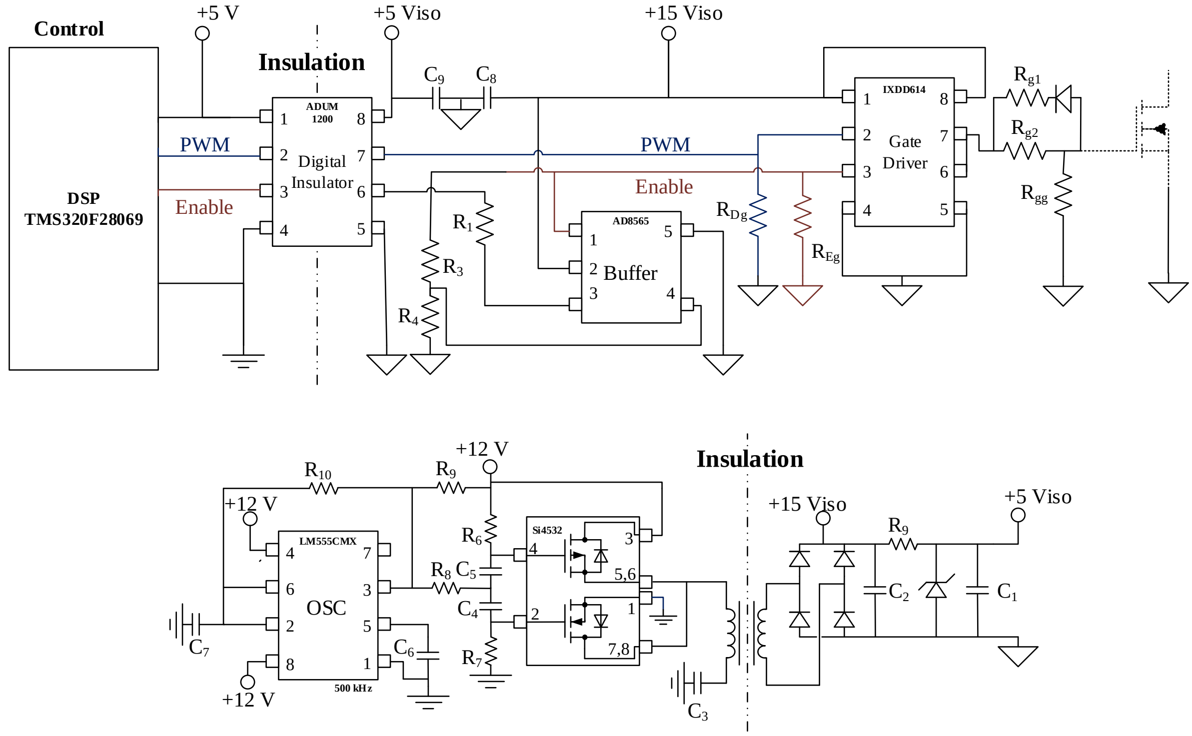

Fig. 6: Circuit used on the MOSFET gate drivers.

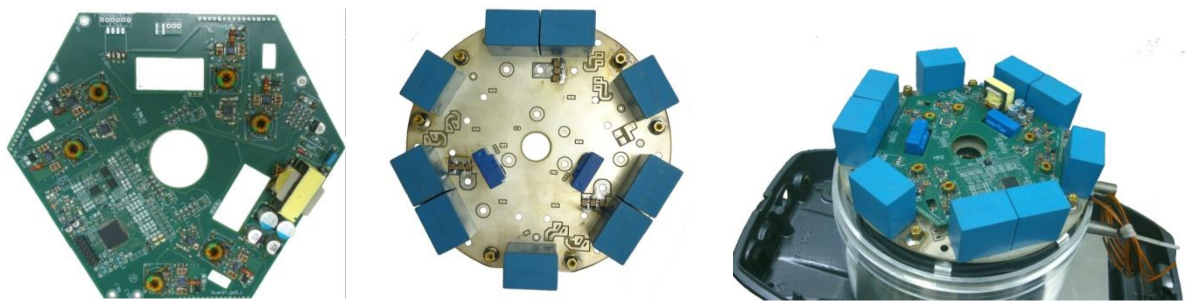

(a) PCB control&command; (b) PCB power; (c) assembled electric power train.

Fig. 7: VSI printed circuit boards.

2.2 Simulation Results

Fig. 8 presents the main waveforms obtained in a circuit simulator for operation of the VSI at rated power (10.5 kW), speed ≈ 5,000 rpm, torque ≈ 18 Nm (≈ 85 A rms per phase), u_{Bat} = 96 V and 10 kHz switching frequency. Fig. 8(a) shows the PMSM stator currents, where it is shown operation with zero d-axis current vector control and low current THD (under 2%). Fig. 8(d) presents the line-to-line voltage (u_{ab}).

Tab. II summarizes the main loss coefficients extracted from the MOSFET datasheet and the semiconductor loss calculation for the simulated operating condition shown in Fig. 8.

Tab. II- Main specifications of the voltage source inverter and semiconductor power losses calculations.

Output power, P_o	10.5 kW
Input voltage, u_{Bat}	75 .. 127 V
Switching frequency (f_s)	8 kHz
MOSFET on-state resistance (at 125 °C), R_{DSon}	8.4 mΩ
MOSFET total switching energy coefficients	a_S = 42.93x10^{-9} J/A^2 b_S = 4.8x10^{-6} J/A c_S = 369.1x10^{-6} J U_m = 133 V
Single MOSFET conduction losses (P_o = 10.5kW and u_{Bat} = 127 V, M = 0.873)	33.455 W
Single MOSFET switching losses (P_o = 10.5kW and u_{Bat} = 127 V, M = 0.873, f_s = 8 kHz)	4.19 W
Total semiconductor loss and efficiency (P_o = 10.5kW and u_{Bat} = 127 V, M = 0.873, f_s = 8 kHz)	226.3 W / 97.84 %

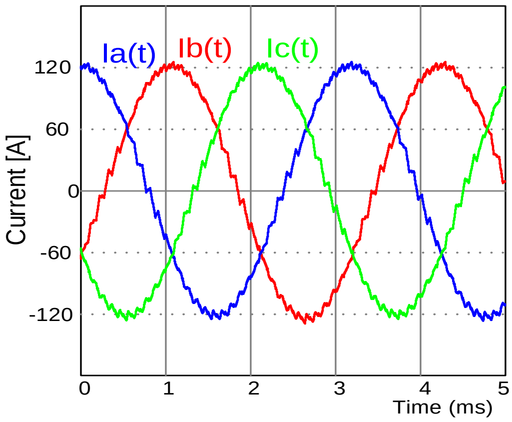

(a) line input currents;

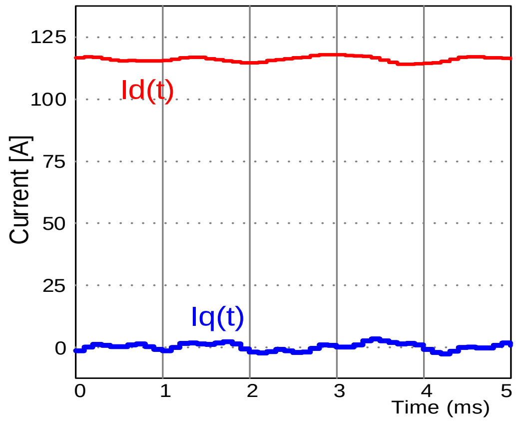

(b) dq0 currents;

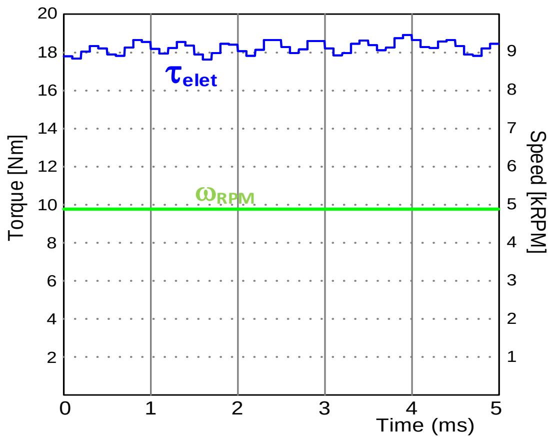

(c) torque and speed

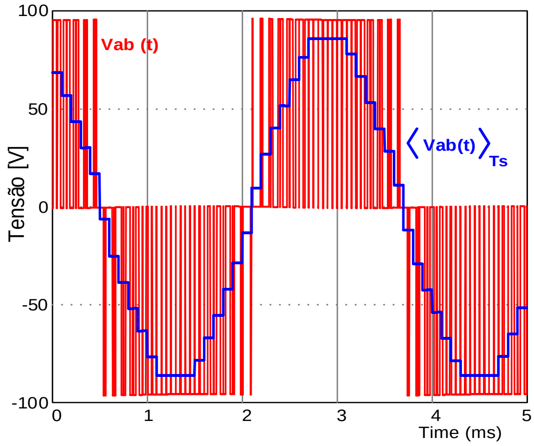

(d) line voltage.

Fig. 8: Main waveforms for the VSI.

3 Water Cooling System

A highly compact propulsion system is derived by using a tailor-made heat sink composed of a cool plate attached to one side of the developed PMSM and with the other side attached to the inverter MOSFET modules (cf. Fig. 9). The mechanical dimensions of this plate match those of the machine in a way that, when covered, the integrated motor drive looks like a cylinder with a diameter of 24 cm and a length of 21.3 cm. The proposed design can directly replace the internal combustion engine in the power head of a commercial outboard motor, from where the water is taken (directly from the sea or lake).

(a) concept; (b) final design.

Fig. 9: Proposed water cooled heat sink and power inverter modules.

4 Experimental Results

In order to maximize the power density of the constructed drive system a sandwich like structure is selected as can be seen in Fig. 2(c). Two printed circuit boards are used for the inverter, one for the power stage and another for the DSP control and command circuits. This is done in order to use PCB's with different copper thicknesses and technologies, e.g. the power board is designed with double layer 250µm (8Oz) PCB to handle the VSI high currents.

Fig. 10 shows the preliminary experimental waveforms obtained with the built converter under low load (Po < 1 kW). As the command and control strategy were devised striving for simplicity, tradeoffs had to be made. One example is the excitation of the PMSM current harmonics which is shown in the FFT of ia(t) in Fig. 11. Given that no correction technique is used [7, 8] the PMSM's trapezoidal back-emf (BEMF) might lead to such consequence [9].

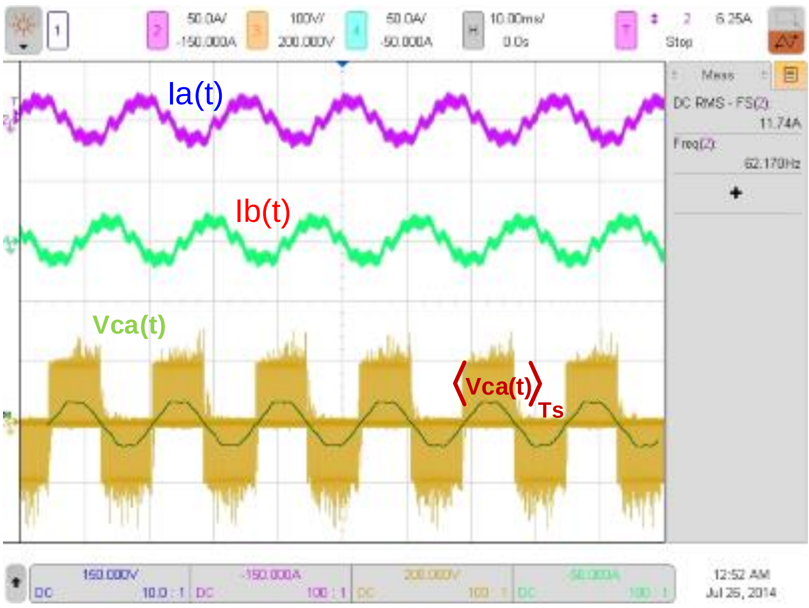

Fig. 10: PMSM waveforms: input voltage and currents.

It is worth mentioning that as the load increases so does the BEMF and the line currents will resemble the BEMF's shape that, in turns, reduces the flux of reactive power. The ripple torque, however, remains present.

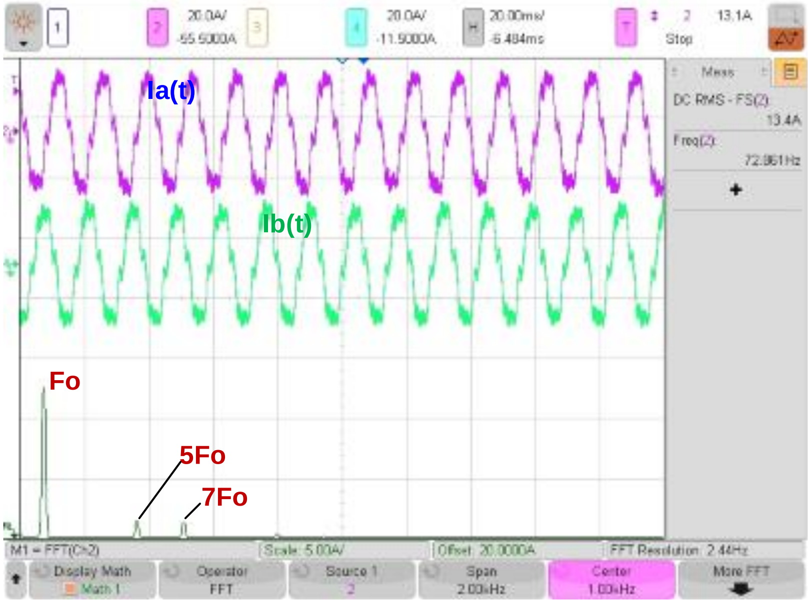

Fig. 11: Phase current harmonics.

It is important to point out that because of the circuitry parasitic inductances and capacitances during the switching transition the switches are prone to over voltages which could be well above the battery voltage level. This can be seen in Fig. 12. Although well below the switches breakdown voltage, the voltage oscillations across the MOSFETs are to be suppressed in the final prototype with the help of additional clamping circuits.

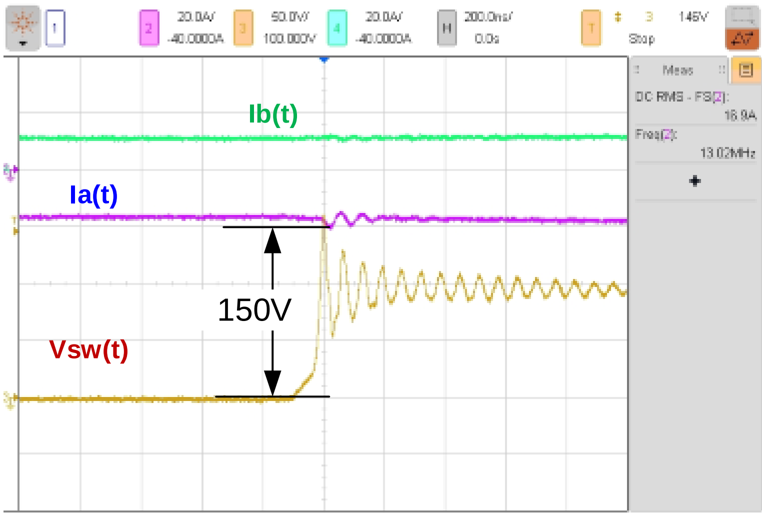

Fig. 12: MOSFET overvoltage – Dead time 2µs.

5 Acknowledgement

This work was developed within the R&D Program framework of Tractebel Energia S.A. and Itá Energética S.A. according to the Brazilian Electrical Energy National Agency (ANEEL) regulation. The authors also express their gratitude to the Brazilian National Council for Scientific and Technological Development (CNPq) for the interest and financial support given in this research project.

6 Conclusions

This work has presented the research performed towards the development of the main components of an integrated motor drive system, which fits directly into the power head of an outboard motor boat. Preliminary experimental results have shown that in a near future a fully functional integration will be ready to be used in an all-electric boat.

7 References

1. Takamasa, T., et al. *Quick charging plug-in electric boat “RAICHO-I”*. in *Electric Ship Technologies Symposium (ESTS), 2011 IEEE*. 2011.
2. Bolognani, S., A. Faggion, and L. Sgarbossa, *High efficiency multidrive system for a hybrid electric catamaran with submersed pm synchronous motors*, in *18th Int. Conf. Electr. Machines (ICEM)*2008: Vilamoura, Portugal. p. 1-5.
3. Chan, C.C., *The state of the art of electric and hybrid vehicles.* Proceedings of the IEEE, 2002. **90**(2): p. 247-275.
4. Mizukoshi, Y., et al., *Power Conversion Apparatus and Motor Drive System*, in *US Patent*, U.S. Patent, Editor 2011, Nissan Motor Co., Ltd, Yokohama (JP): US. p. 13.
5. Nakano, M., Y. Asao, and I. Sonoda, *Motor Drive Apparatus*, 2013, Mitsubishi Electric Corporation: US. p. 26.
6. Peterson, G.A., D.E. Hilton, and M.W. Major, *Integrated Direct Drive Motor and Control*, 2013, Nidec Motor Corporation: US. p. 13.
7. Chapman, P.L., S.D. Sudhoff, and C.A. Whitcomb, *Optimal current control strategies for surface-mounted permanent-magnet synchronous machine drives.* Energy Conversion, IEEE Transactions on, 1999. **14**(4): p. 1043-1050.
8. Panda, S.K., X. Jian-Xin, and Q. Weizhe. *Review of torque ripple minimization in PM synchronous motor drives*. in *Power and Energy Society General Meeting - Conversion and Delivery of Electrical Energy in the 21st Century, 2008 IEEE*. 2008.
9. Jahns, T.M. and W.L. Soong, *Pulsating torque minimization techniques for permanent magnet AC motor drives-a review.* Industrial Electronics, IEEE Transactions on, 1996. **43**(2): p. 321-330.